Experimental Study on Pile Foundations having Batter Piles Subjected to Combination of Vertical and Horizontal Loading at 1-g Field

Anh-Tuan Vu[1], Tatsunori Matsumoto[2], Shun-ichi Kobayashi[3] and Shinya Shimono[4]
[1,2,3,4]*Graduate School of Natural Science and Technology, Kanazawa University, Japan*
[1]*Department of Civil Engineering, Le Quy Don Technical University, Vietnam*
[1]*E-mail:* vuanhtuan@mta.edu.vn
[2]*E-mail:* matsumoto@se.kanazawa-u.ac.jp
[3]*E-mail:* koba@se.kanazawa-u.ac.jp
[4]*E-mail:* shimono@se.kanazawa-u.ac.jp

ABSTRACT: In this study, the behaviours and resistance mechanisms of pile foundations having batter piles were investigated through a series of vertical load tests and combination load tests on model foundations in dry sand ground at 1-g field. Pile foundation models consisting of 3 piles and 6 piles, with or without batter piles, were used in the experiments. The model pile was close-ended pipe with a length of 255 mm and an outer diameter of 20 mm. Dry silica sand having a relative density, D_r, of about 82% was used for the model ground throughout the experiments. Triaxial CD tests of the sand were carried out to obtain the mechanical properties and to investigate the behaviour of the sand. The results indicate that the piled raft having batter piles is the most effective to increase the resistances (in both vertical and horizontal directions) and reduce the inclination.

KEYWORDS: Piled raft, Pile group, Batter pile, Dry sand, Model test

1. INTRODUCTION

Pile foundations having batter piles have been adopted in practice for structures subjected to large horizontal loads such as bridges or offshore structures. In practical conditions, these pile foundations carry not only vertical loads but also horizontal loads such as wind loads, wave loads and earthquakes.

Number of studies on batter piles were reported, e.g. Ghasemzadeh and Alibeikloo (2011), Goit and Saitoh (2013), Isam et al. (2012), and Sadek and Isam (2004). However, the researches investigated the behaviours of pile groups with batter piles (Ghasemzadeh and Alibeikloo, 2011; Isam et al., 2012; Sadek and Isam, 2004) or single batter piles (Goit and Saitoh, 2013). Moreover, these researches investigated the foundation behaviours subjected to vertical loading alone or horizontal loading alone. Therefore, the resistance mechanisms of foundations having batter piles subjected to combination loads have not been fully understood.

Applications of piled raft foundations to buildings are increasing in the world to reduce average and/or differential settlement, e.g. Katzenbach et al (1998), Poulos and Davids (2005), Poulos et al. (2011), and Yamashita et al. (2011). Experimental studies as well as numerical analyses on piled raft foundation having vertical piles alone have been conducted, e.g. Randolph (1994), Horikoshi and Randolph (1998), Horikoshi and Randolph (1999), Horikoshi et al. (2003), Matsumoto et al. (2004), Reul (2004), Sawada and Takemura (2014), Unsever et al. (2014), Vu et al. (2014), Hamada et al. (2015) and Unsever et al. (2015).

Unsever et al. (2014) carried out the experimental study on pile group and piled raft models having only vertical piles subjected to combination of vertical and horizontal load at 1-g field. Sawada and Takemura (2014) studied on pile group and piled raft models having only vertical piles subjected to combination load using a centrifuge device.

There is few experimental study on behaviours of piled rafts having batter piles. Hence, in this research, behaviours and resistance mechanisms of pile groups and piled rafts having batter piles were investigated through a series of load tests (vertical load tests and combination load tests) on foundation models in dry sand ground at 1-g field. Pile foundation models consisting of 3 piles and 6 piles, with or without batter piles, were used in the experiments. A reason why the two types of the model foundations were used is to investigate also the interaction of the raft and the piles through the ground.

It should be noted that the small-sized experiments were carried out at 1-g field. Hence, the experiments did not aim to simulate the behaviour of a prototype, but to investigate the influence of inclusion of batter piles on the piled raft or the pile group subjected to combination of vertical and horizontal loading, and also investigate the resistance mechanisms of the foundations. The results of the experiments are presented and discussed in this paper.

2. OUTLINE OF THE EXPERIMENTS

2.1 Model foundations

Figure 1 shows the foundation models used in the experiments. The foundation models consist of 3 piles or 6 piles (with or without batter piles). They are pile groups (3PG, 3BPG, 6PG and 6BPG) if the raft base is not in contact with the ground surface, while they are piled rafts (3PR, 3BPR, 6PR and 6BPR) if the raft base is in contact with the ground surface.

Close-ended aluminium pipes having a total length of 285 mm, an outer diameter of 20 mm and a wall thickness of 1.1 mm were used for the model piles. The upper 30 mm of the pile is embedded in the raft, resulting in the effective length of 255 mm. Centre-to-centre pile spacing, *s,* is 80 mm, 4 times the pile diameter. The inclination angle of the batter piles is 15 degrees. Young's modulus of the piles, E_p, was estimated from bending tests of the piles. The geometrical and mechanical properties of the model pile are summarised in Table 1. In order to obtain axial forces, bending moments and shear forces in the model piles during load tests, strain gauges were arranged on the pile shafts (Figure 2). The piles were covered with the silica sand particles in order to increase the shaft resistance.

The rafts were made of duralumin with the dimensions as shown in Figure 1 and can be regarded as rigid. The sand particles were adhered on the raft base surface to increase the friction between the raft and the ground during horizontal loading.

2.2 Model ground

The soil used for model ground in this study is a dry silica sand having the properties shown in Table 2. The model ground with a relative density, D_r, of about 82% (ρ_d = 1.533 t/m^3) was prepared in a soil box having dimensions of 800 mm in length, 500 mm in width and 530 mm in depth (see Figure 3). In order to control the density of the model ground, the model ground was prepared by 11 layers (10 layers of 50 mm and 1 layer of 30 mm).

Table 1 Geometrical and mechanical properties of the model pile

Properties	Value
Outer diameter, D (mm)	20
Wall thickness, t (mm)	1.1
Effective length from raft base, L (mm)	255
Young's modulus, E_p (N/mm^2)	70267
Poisson's ratio, ν	0.31

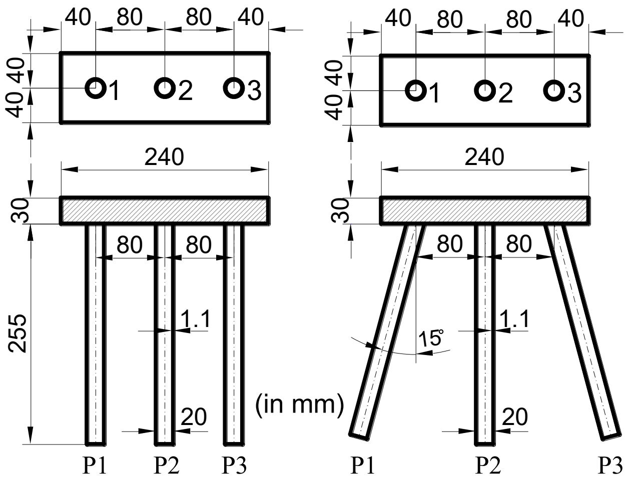

a) 3PG and 3PR (b) 3BPG and 3BPR

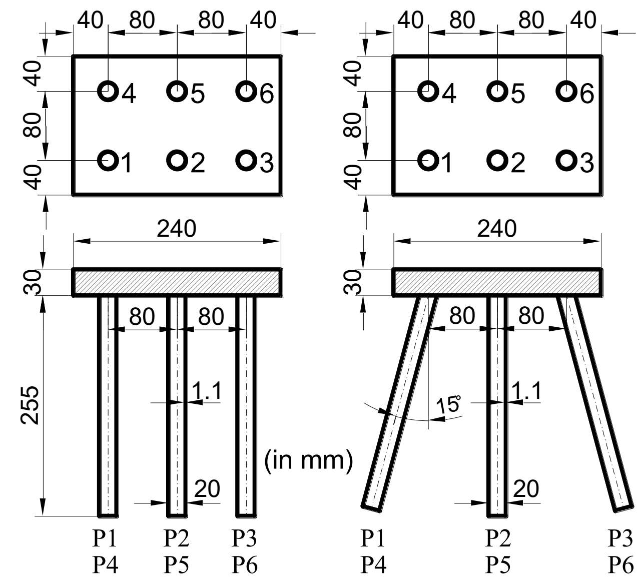

c) 6PG and 6PR (b) 6BPG and 6BPR

Figure 1 Dimensions of the foundation models

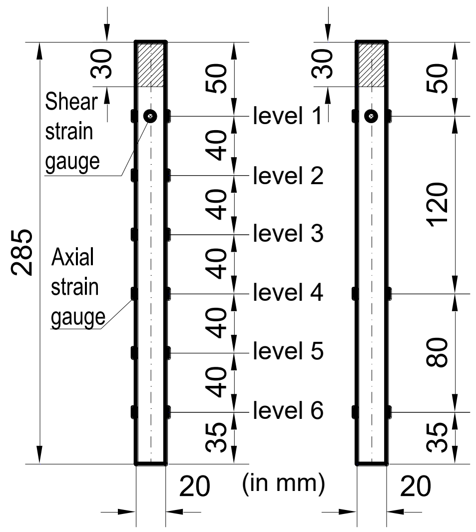

a) P1, P2 and P3 b) P4, P5 and P6

Figure 2 Model piles with strain gauge instrumentation

In each layer, the sand was poured and compacted by tapping so that the target relative density of 82% was attained. The sequence of the preparation of the model ground is summarised as follows:

1) Place 5 soil layers of 50 mm (total height is 250 mm) one by one and compact until an intended relative density of 82%.
2) Fix temporarily the model foundation to the planned position by the help of steel bars and clamps.
3) Place and compact 5 more soil layers of 50 mm and 1 more soil layer of 30 mm until the total height of the model ground of 530 mm is obtained.

Table 2 Properties of the sand used for model ground

Property	Value
Density of soil particle, ρ_s (t/m^3)	2.668
Maximum dry density, ρ_{dmax} (t/m^3)	1.604
Minimum dry density, ρ_{dmin} (t/m^3)	1.269
Maximum void ratio, e_{max}	1.103
Minimum void ratio, e_{min}	0.663

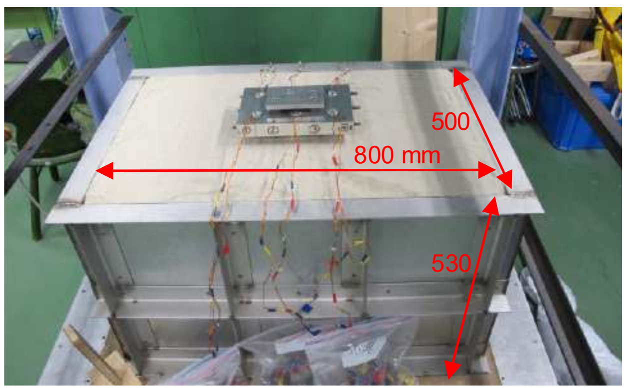

Figure 3 Dimensions of the soil box

2.3 Loading methods

The loading methods employed are similar to those in Unsever, et al. (2014).

In vertical load tests (Figure 4), the load was applied by the help of a screw jack with a constant displacement rate of about 2 mm/min. The vertical load was measured by a load cell placed on the centre of the raft. The vertical displacement of the foundation was recorded by 4 dial gauges arranged at the corners of the raft.

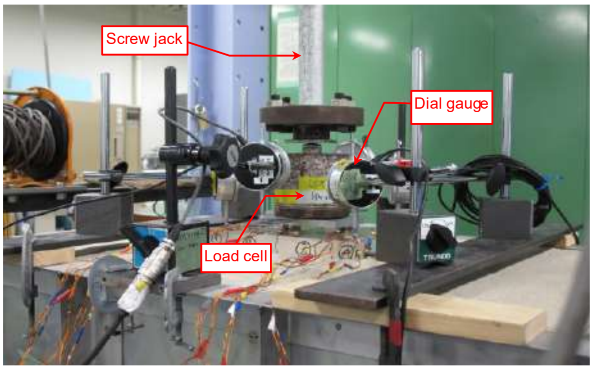

Figure 4 Experiment setup with measuring instruments in vertical load tests

Figure 5 shows the schematic illustration of the experiment setup in a combination load test. Vertical load was applied by placing lead plates of about 600 N and 1200 N on the raft in the cases of 3-pile pile foundations and 6-pile pile foundations, respectively, to simulate the dead weight of the super structure. After that, cyclic static horizontal load was applied at the raft in longitudinal direction of the raft by means of winches and pulling wires (see Figure 6). Hence, the foundations would be subjected to combination of vertical load and horizontal load during the horizontal loading stage. The horizontal load was measured by 2 load cells (LC-R and LC-L) arranged in the right (positive) direction and in the left (negative) direction. Both the horizontal and vertical displacements of the foundations were recorded by horizontal and vertical dial gauges.

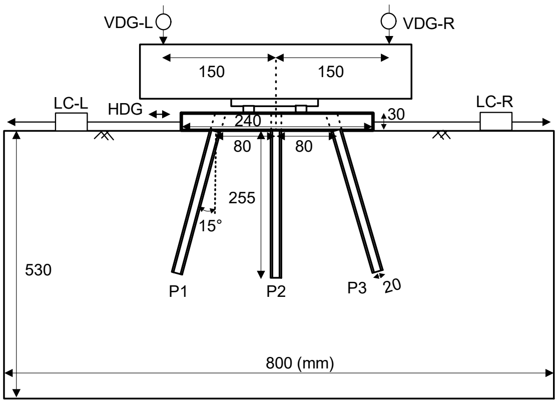

Figure 5 Schematic illustration of a combination load test

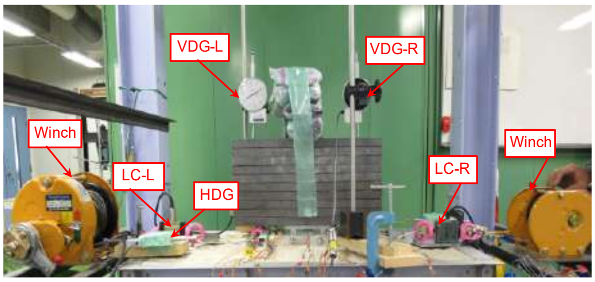

Figure 6 Experiment setup with measuring instruments in combination load tests

3. EXPERIMENTAL RESULTS

3.1 Cone Penetration Test

The uniformity of the model grounds in all the tests was examined through tests using a miniature cone penetrometer with a diameter of 20 mm and an apex angle of 60 degrees. The results of the Cone Penetration Tests (CPTs) of the model grounds are shown in Figure 7. It is seen that the model grounds are almost uniform in plane and the cone tip resistance, q_c, increases almost linearly with depth in all the tests.

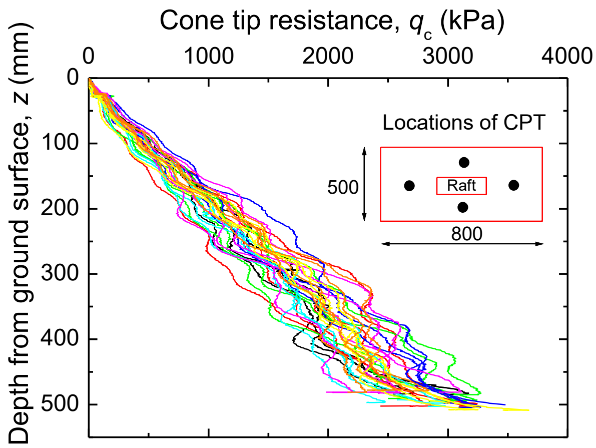

Figure 7 The results of Cone Penetration Tests

3.2 Triaxial test

A series of triaxial CD tests of the sand having D_r = 82% were conducted under different confining pressures, p_0 = 7, 17, 27, 50, and 100 kPa, in order to obtain the mechanical properties and to investigate the behaviour of the sand. In addition, a cyclic CD test was conducted under p_0 = 100 kPa.

The test results, axial strain ε_a vs. deviatoric stress q, and ε_a vs. volumetric strain ε_{vol}, are shown in Figure 8a and Figure 8b, respectively. It is seen from Figure 8a that the stiffness increases with increasing p_0. Non-linearity and post-peak softening behaviours are observed from the stress-strain relations. It was estimated from the experimental results that the peak internal friction angle, ϕ_p', is 42.8 degrees while the residual internal friction angle, ϕ_r', is less than 35 degrees. It is seen from Figure 8b that dilatancy becomes smaller as p_0 increases and dilatancy angle, Ψ, is not constant but decreases with increasing ε_a.

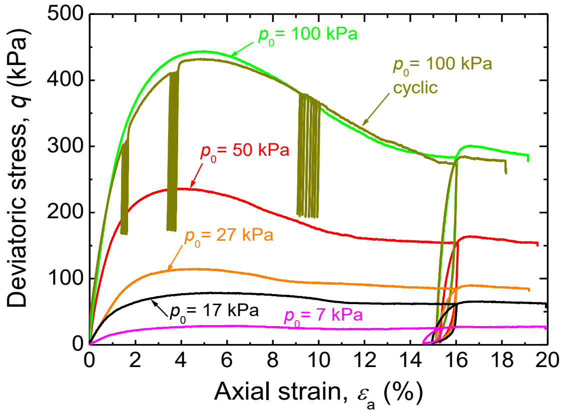

(a) Axial strain ε_a versus deviatoric stress q

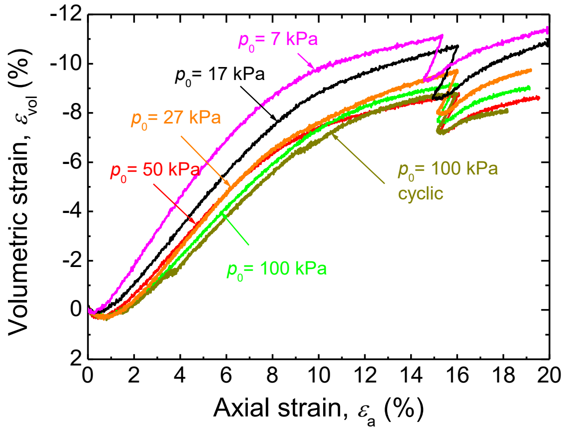

(b) Axial strain ε_a versus volumetric strain ε_{vol}

Figure 8 The results of triaxial CD tests of the sand

3.3 Vertical load tests

Figure 9 shows the load-settlement curves in the cases of the 3-pile foundations (Figure 9a) and the 6-pile foundations (Figure 9b). The results in the cases of the 3-pile foundations indicate that 3BPR has the highest resistance and stiffness followed by those of 3PR, 3BPG and 3PG, subsequently. Similarly, 6BPR has the highest resistance and stiffness followed by those of 6PR, 6BPG and 6PG, subsequently, in the cases of the 6-pile foundations. It is obvious that the resistances of the piled rafts are much higher than those of the corresponding pile groups, and the resistances of the foundations are considerably improved by inclusion of batter piles, in both types of piled raft and pile group.

The positive effect of batter piles in reducing settlement is shown obviously from comparison of the curves of 3PG and 3BPG. For instance, the settlement of 3PG is 1.3 mm at a vertical load V = 1000 N while the settlement of 3BPG is only 0.7 mm, resulting in 46% decrease of the settlement. The similar effect is also seen from comparison of the curves of 6PG and 6BPG. This positive effect is also notable in the cases of the piled rafts although it is not as significant as it is in the cases of the pile groups.

Please notice here that the positive effect of the inclusion of batter piles mentioned above may not be directly applied in actual piles. In general, it has been thought that batter piles are not effective for vertical load comparing with vertical piles. Because the batter pile will be bent in the direction perpendicular to the axial direction by vertical loading, a foundation with batter piles may result in larger settlement if the pile does not have enough bending rigidity. Vu et al (2016) discussed a similitude for experiments at 1-g field based on the similitude proposed by Iai (1989). Vu et al (2016) showed that, in the case of scale ratio (prototype scale/model scale) of λ = 30 for an example, the bending rigidity, EI, and longitudinal rigidity, EA, of a prototype pile are 4.35 and 0.41 times those of a concrete pile ($E = 3\times10^6$ kPa) having a diameter of 0.6 m and a length of 7.65 m. That is, the model pile used in the experiments is regarded as a "short pile" condition.

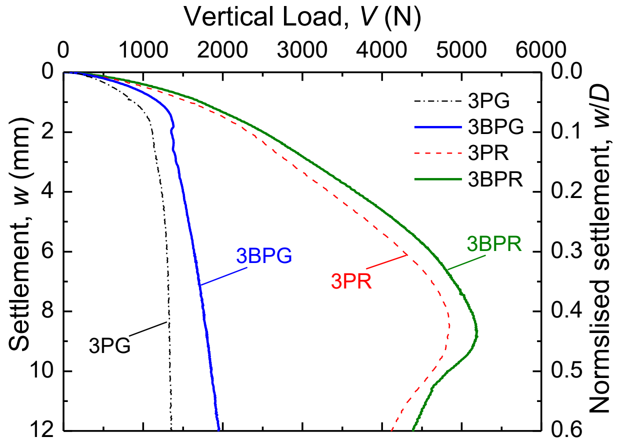

(a) 3-pile foundations

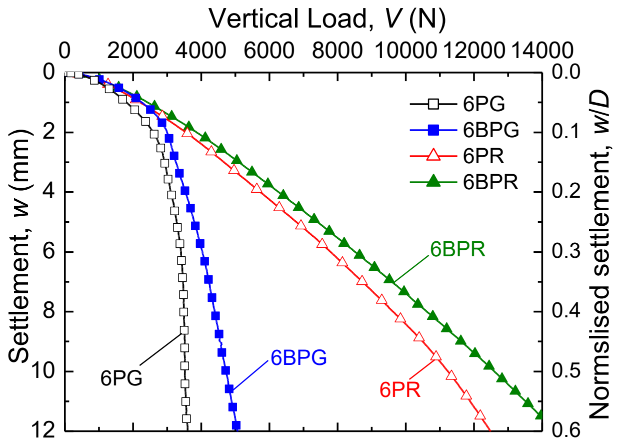

(b) 6-pile foundations

Figure 9 Load-settlement curves of the foundation models

The vertical resistances by the piles and the rafts in the cases of 3PR and 6PR are shown in Figure 10. The proportions of vertical load carried by the each component are given in Figure 11. It is seen from Figure 10 and Figure 11 that the load carried by the raft in the case of 3PR is very small at the early loading stage. After that the raft load increases to the peak value and then decreases with the increase of the displacement, resulting in a softening behaviour. Note that the softening behaviour was also observed in the triaxial tests of the sand.

The similar trend that the load carried by the raft is very small at the early loading stage and then increases with increasing w, is also seen in the case of 6PR, but the softening behaviour was not observed until w reached 12 mm. More loading was not possible, because the load exceeded the capacity of the experiment devices.

It could be explained that imperfect contact between the raft and the ground surface is a reason why most of the total load is carried by the piles at the very early loading stage. As mentioned in Section 2.2 on the sequence of the model ground preparation, the top soil layer was compacted after fixing the foundation temporarily. Hence imperfect contact between the raft and the ground surface was inevitable. It is also a reason why the raft resistance of 6PR is not so larger than that of 3PR at the initial loading stage, as shown in Figure 10.

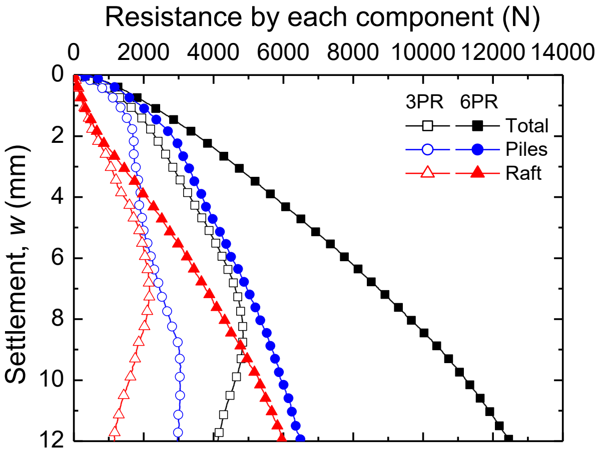

Figure 10 Load-settlement curves in cases of 3PR and 6PR

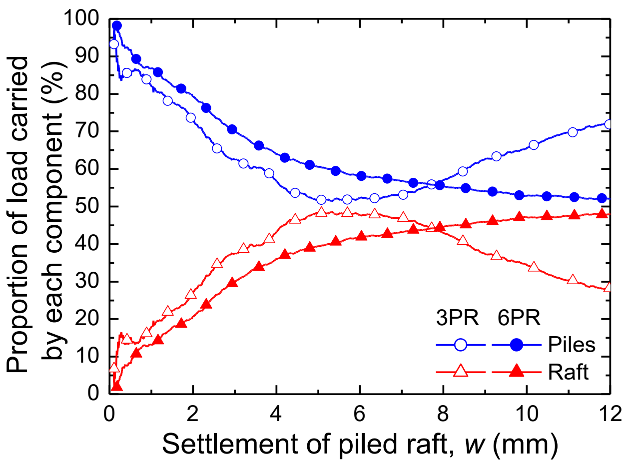

Figure 11 Proportions of vertical load carried by the pile component and the raft component in the cases of 3PR and 6PR

Figures 12 and 13 show the axial force distributions along the pile P1 at various normalised settlements, w/D = 0.01, 0.02, 0.05, 0.20, 0.40 and 0.60, for the 3-pile foundations (3PG, 3BPG, 3PR and 3BPR) and the 6-pile foundations (6PG, 6BPG, 6PR and 6BPR), respectively. It is noticed that P1 is one of the batter piles in the batter pile foundations (3BPG, 3BPR, 6BPG and 6BPR).

It can be seen that the axial forces of the pile P1 in the batter pile groups (3BPG and 6BPG) are larger than those of the corresponding pile groups without batter piles (3PG and 6PG) at any normalised settlement. In the cases of the piled rafts, the differences of axial forces (comparison of 3BPR and 3PR, and comparison of 6BPR and 6PR) are not as considerable as those in the cases of the pile groups. It is interesting to notice that the axial forces in the piled rafts are larger than those in the corresponding pile groups, especially at large normalised settlements. This is due to effect of load transferred from the raft base to the ground. The load transferred from the raft base causes the increase of the stress level in the ground, resulting in the increase of stiffness and strength as indicated in the triaxial test results.

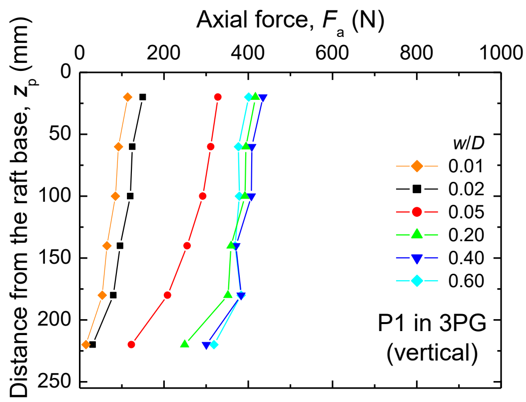

(a)

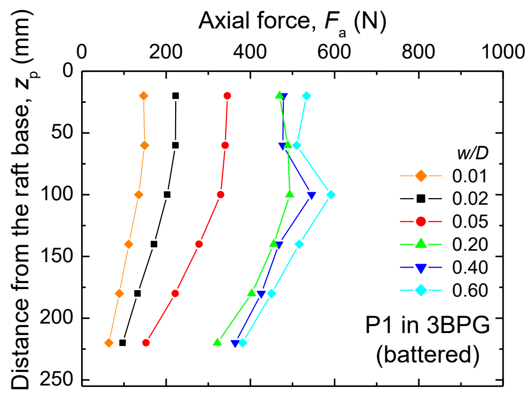

(b)

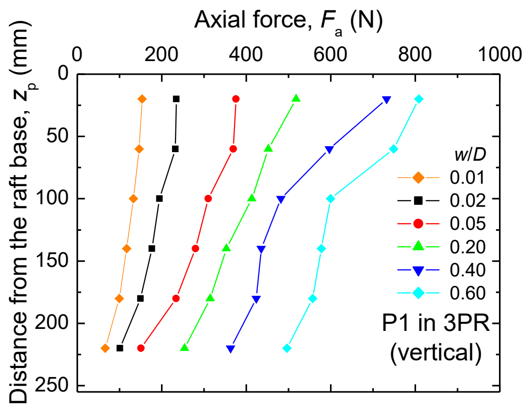

(c)

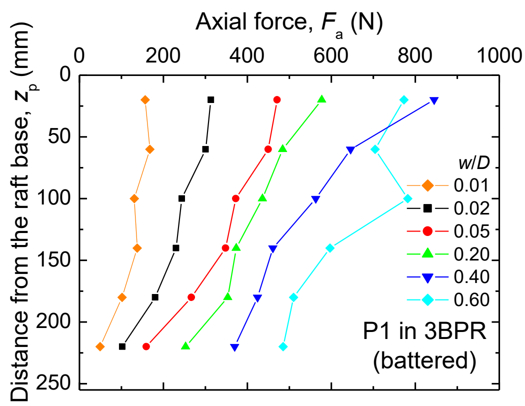

(d)

Figure 12 Axial force distributions along pile shaft of P1 in the cases of 3PG, 3BPG, 3PR and 3BPR

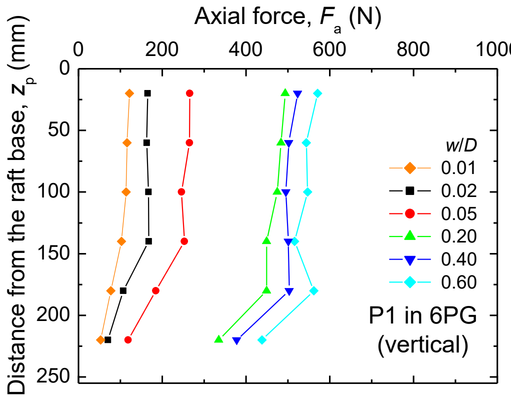

(a)

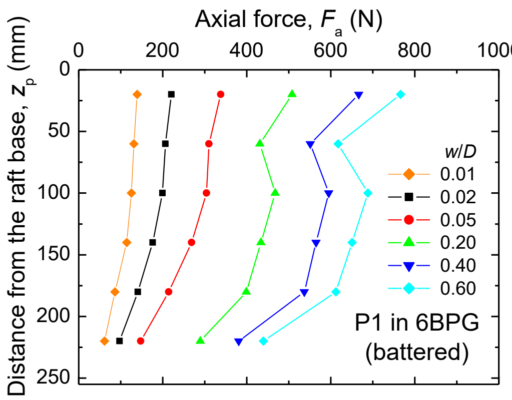

(b)

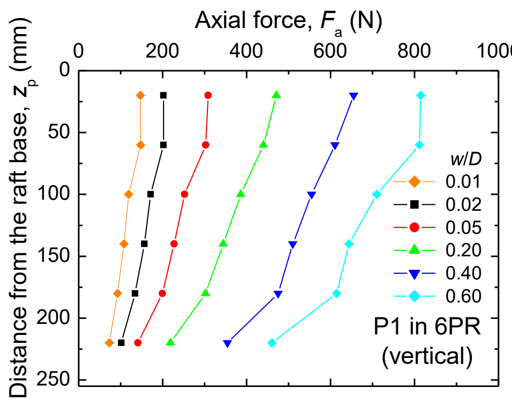

(c)

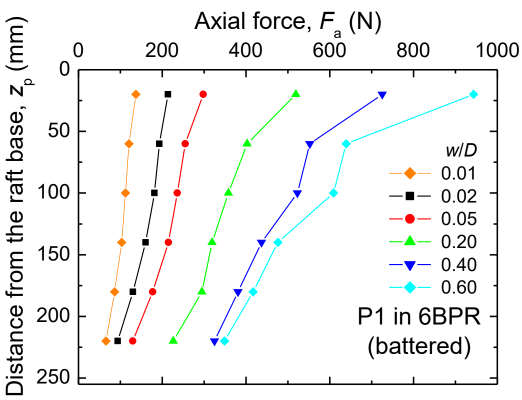

(d)

Figure 13 Axial force distributions along pile shaft of P1 in the cases of 6PG, 6BPG, 6PR and 6BPR

In a similar way, Figures 14 and 15 show the bending moment distributions along the pile P1 at various normalised settlements, w/D = 0.01, 0.02, 0.05, 0.20, 0.40 and 0.60, in the cases of the 3-pile foundations and the 6-pile foundations, respectively. It is seen that larger bending moments are generated in the pile of the batter pile foundations (3BPG, 3BPR, 6BPG and 6BPR) compared to those of the corresponding pile foundations without batter piles (3PG, 3PR, 6PG and 6PR).

Let us here briefly discuss the interactions observed in the vertical load tests. Load-settlement curves for 6PG, 6BPG, 2×3PG and 2×3BPG are given in Figure 16. It is seen that the resistances of the 6-pile pile groups are almost equal to two times the resistances of the 3-pile pile groups when settlement is smaller than 1.5 mm. When settlement exceeds 1.5 mm, the resistances of the 6-pile pile groups are considerably larger than two times the resistances of the 3-pile pile groups. It is interesting to find that the axial forces are similar between 3PG and 6PG, and also similar between 3BPG and 6BPG at the small normalised settlements, w/D = 0.01, 0.02 and 0.05 (see Figures 12 and 13). At the large normalised settlements, w/D = 0.2, 0.4 and 0.6, larger axial forces, mainly caused by larger tip resistance, are generated in 6-pile pile groups compared to those in 3-pile pile groups. This is the reason for the larger resistance of the 6-pile pile groups compared to two times the resistances of the 3-pile pile groups.

Figure 17 shows load-settlement curves for 6PR, 6BPR, 2×3PR and 2×3BPR. In contrast to the results in the cases of the pile groups, the resistances of 6PR and 6BPR are smaller than 2×3PR and 2×3BPR, correspondingly. The results in Figure 10 indicate that the load carried by the 6 piles in 6PR is approximately two times of the load carried by the 3 piles in 3PR. Meanwhile, the load supported by the raft in 6PR is considerable smaller than two times of the load carried by the raft in 3PR until w attains about 8 mm. That is the reason why the resistances of 6PR and 6BPR are smaller than 2×3PR and 2×3BPR until w attains about 8 mm.

3.4 Horizontal load tests

Figure 18 shows the relationships of horizontal load, H, and normalised horizontal displacement, u/D, in the cases of 3PG, 3BPG, 3PR and 3BPR. Figure 19 shows the results of 6PG, 6BPG, 6PR and 6BPR.

The results from both Figure 18 and Figure 19 indicate clearly that the piled rafts have much higher horizontal resistances than the corresponding pile groups. It is also seen that the resistances of the foundations are effectively improved by inclusion of batter piles in both cases of piled raft (BPR) and pile group (BPG).

It is confirmed from the above results that piled raft having batter piles is the most effective to increase the resistances, in both vertical and horizontal directions.

Figure 20 shows comparisons of inclination of the raft during cyclic horizontal loading between 6PG and 6BPG (Figure 20a), and between 6PR and 6BPR (Figure 20b). The inclination increases almost linearly with the increase of normalised horizontal displacement in all cases. The inclination of the raft is suppressed by inclusion of the batter piles, and this effect is more considerable in the case of piled raft.

Figure 21 shows the relationship between the inclination of the raft and horizontal load during the initial loading stage for 6PG, 6BPG, 6PR and 6BPR. The results indicate that the inclinations of the piled rafts are smaller than those of the corresponding pile groups at any given horizontal load.

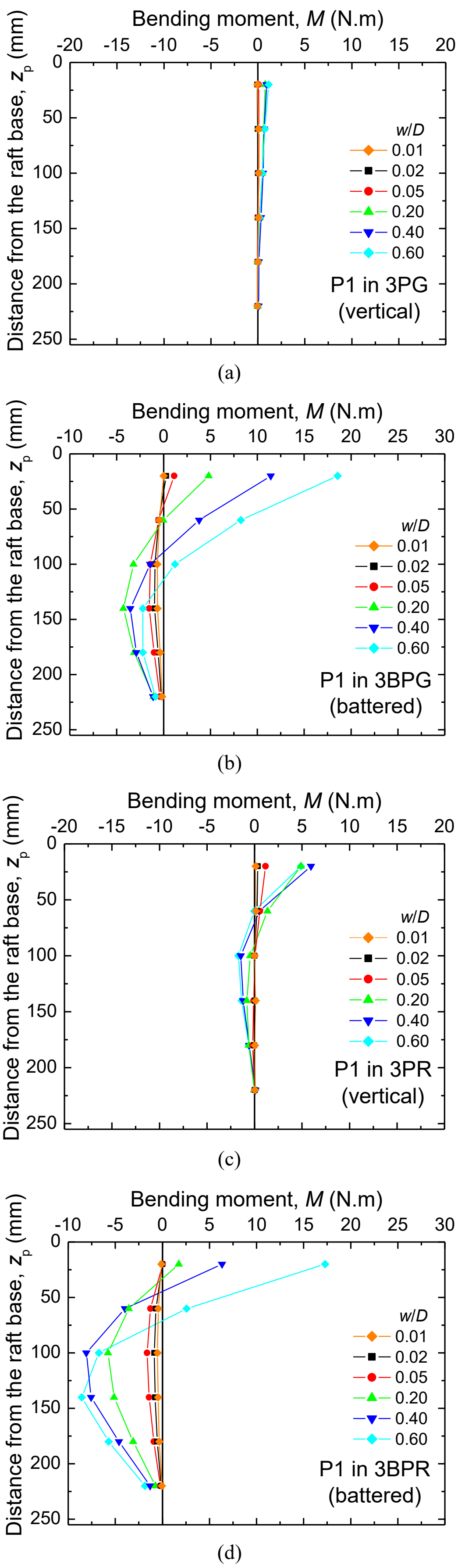

Figure 14 Bending moment distributions along pile shaft of P1 in the cases of 3PG, 3BPG, 3PR and 3BPR

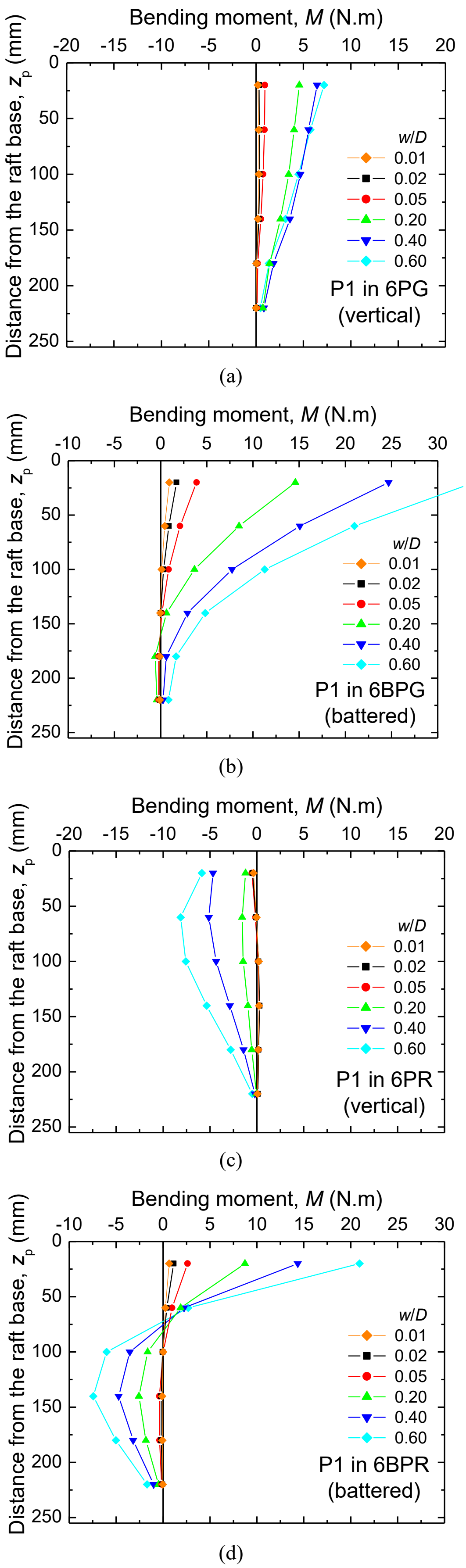

Figure 15 Bending moment distributions along pile shaft of P1 in the cases of 6PG, 6BPG, 6PR and 6BPR

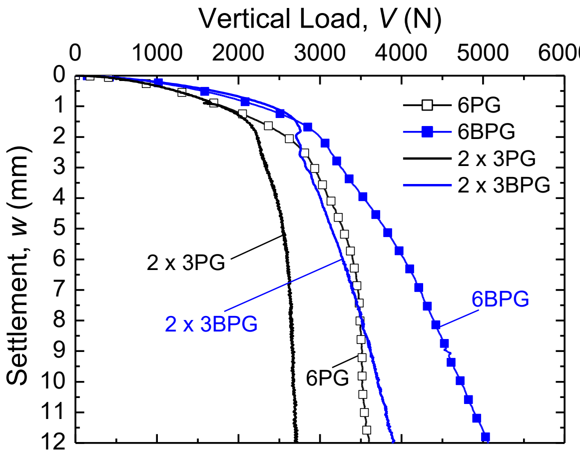

Figure 16 Load-settlement curves for 6PG, 6BPG, 2×3PG and 2×3BPG

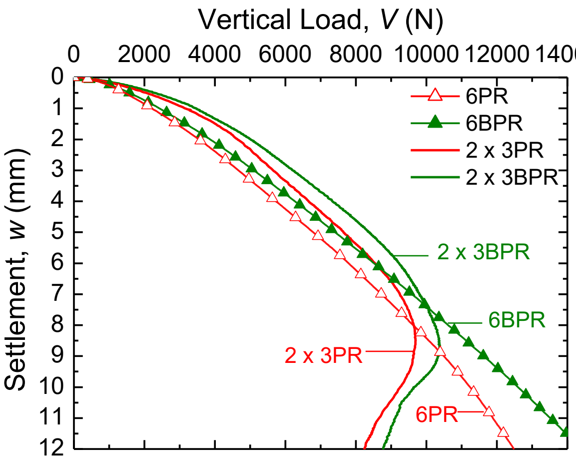

Figure 17 Load-settlement curves for 6PR, 6BPR, 2×3PR and 2×3BPR

Also, the inclinations of the foundations with batter piles are smaller than those of the corresponding pile foundations without batter piles at any given horizontal load. It is worth to notice that the piled raft with batter piles is the most favourable foundation type to reduce the inclination.

Let us here briefly discuss the interactions observed in the horizontal load tests. Horizontal load-horizontal normalised displacement curves for 6PG, 6BPG, 2×3PG and 2×3BPG are given in Figure 22. In a similar way, Figure 23 shows horizontal load-horizontal normalised displacement curves for 6PR, 6BPR, 2×3PR and 2×3BPR. It is seen that the horizontal resistances of the 6-pile foundations are smaller than two times the resistances of the 3-pile foundations, showing non-negligible interaction effects. Numerical analyses will be conducted in future to get more insight into the behaviours of the foundations and to understand more about the interactions of raft, piles and soil.

The axial loads at the pile head carried by the rear piles, the centre piles and the front piles for 3PR, 3BPR, 6PR and 6BPR are given in Figure 24. Here, the axial loads are defined as the axial forces at a top of each pile (20 mm below the raft base). In the cases of 6PR and 6BPR, the axial loads are obtained by taking average values of the axial loads of rear piles (P1 and P4), the centre piles (P2 and P5) and the front piles (P3 and P6).

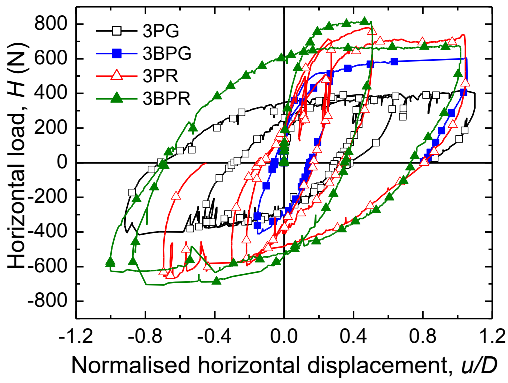

(a) all cycles

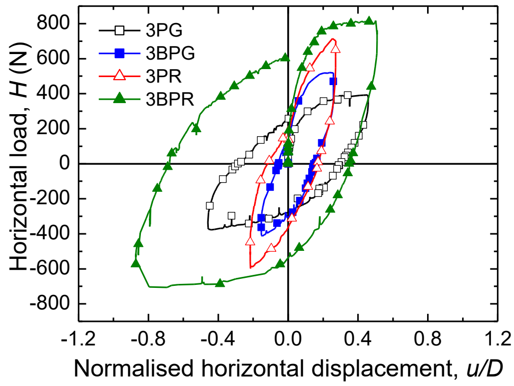

(b) 1st cycle

Figure 18 Horizontal load-normalised horizontal displacement curves for 3PG, 3BPG, 3PR and 3BPR

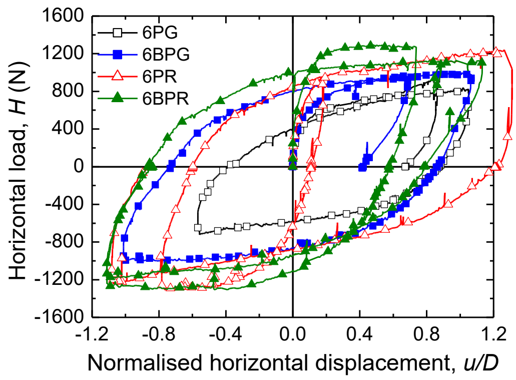

(a) all cycles

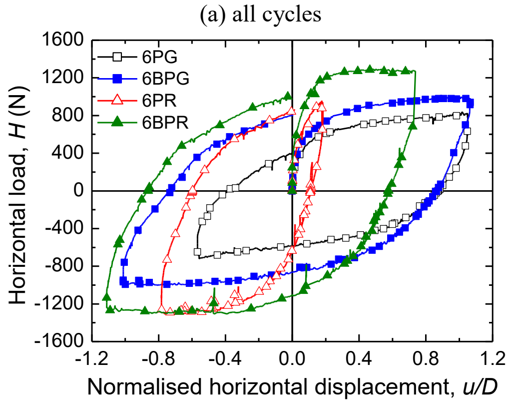

(b) 1st cycle

Figure 19 Horizontal load-normalised horizontal displacement curves for 6PG, 6BPG, 6PR and 6BPR

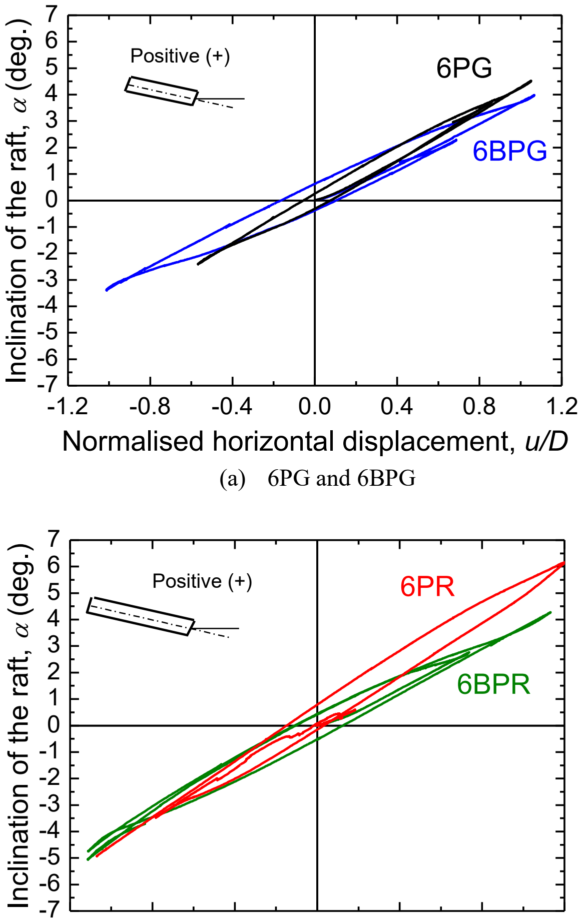

(a) 6PG and 6BPG

(b) 6PR and 6BPR

Figure 20 Inclination of the raft during cyclic horizontal load

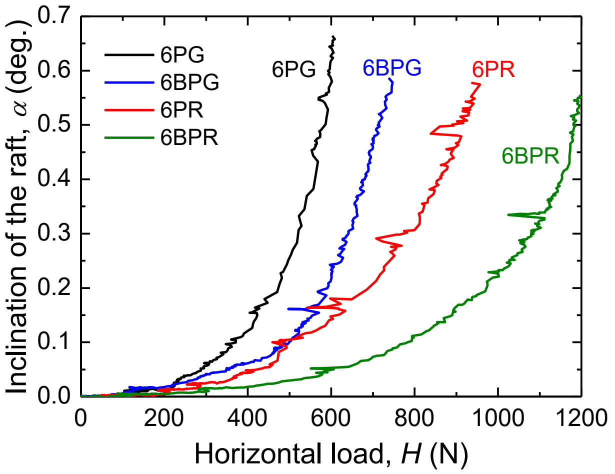

Figure 21 Inclination of the raft vs. horizontal load during the initial loading stage for 6PG, 6BPG, 6PR and 6BPR

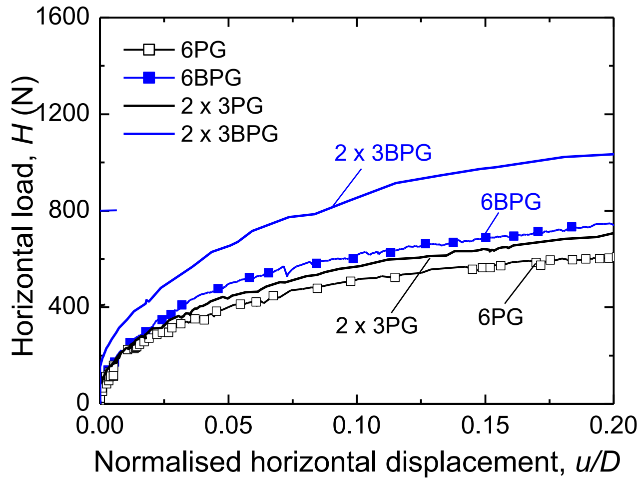

Figure 22 Horizontal load vs. normalised horizontal displacement during initial loading stage for 6PG, 6BPG, 2×3PG and 2×3BPG

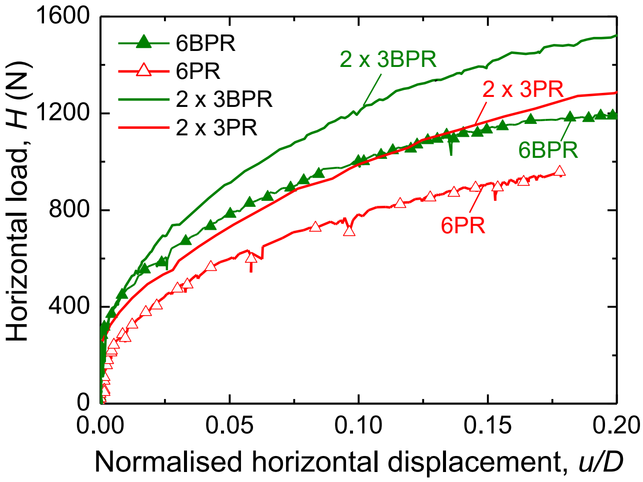

Figure 23 Horizontal load vs. normalised horizontal displacement during initial loading stage for 6PR, 6BPR, 2×3PR and 2×3BPR

In this paper, compression axial force is taken as positive and tension axial force is taken as negative. It can be seen that the curves in the four cases have similar trends, in which the front piles tend to take compression load, meanwhile the centre piles and the rear piles tend to take tension load. Focusing on the load of front piles, it is seen that the loads carried by the front piles (battered pile) in 3BPR and 6BPR are higher than those (vertical pile) in 3PR and 6PR at any given horizontal displacement. As for the rear piles, the loads in 3BPR and 6BPR change from compression into tension more rapidly than those in 3PR and 6PR. Also, the magnitudes of tension load in the cases of 3BPR and 6BPR are higher than those in 3PR and 6PR. The magnitudes of axial forces of the piles in the case of BPR (batter piles) are larger than those in the case of PR (vertical piles), enhancing the horizontal resistance of BPR compare to PR.

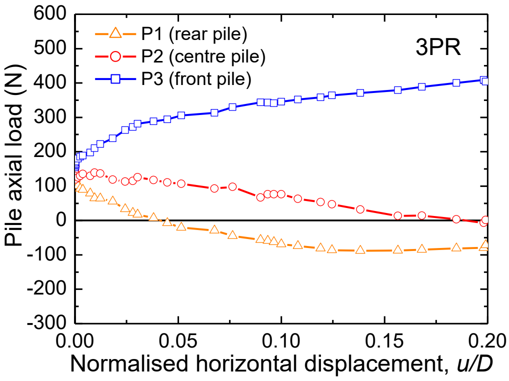

(a) Case of 3PR

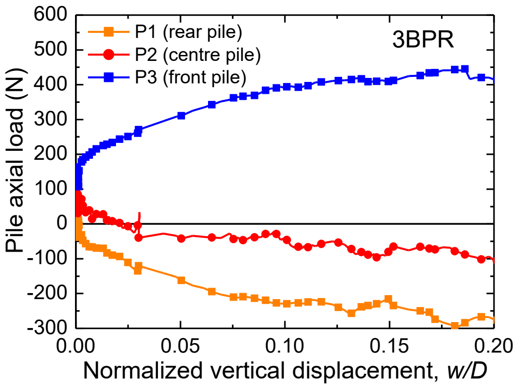

(b) Case of 3BPR

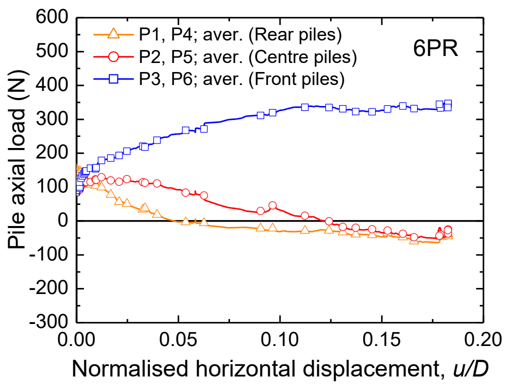

(c) Case of 6PR

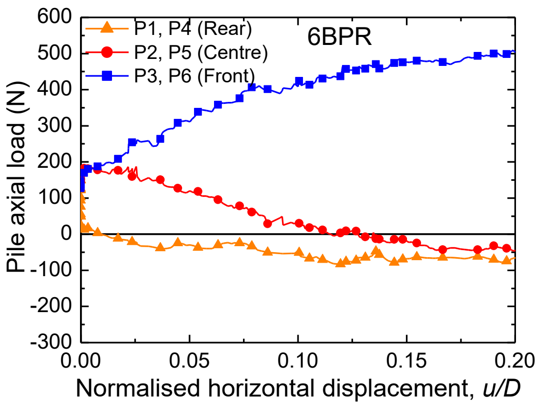

(d) Case of 6BPR

Figure 24 Pile axial load vs. normalised horizontal displacement for 3PR, 3BPR, 6PR and 6BPR

Changes of bending moments with normalised horizontal displacement, u/D, at different levels (see Figure 2) of each pile during horizontal loading are given in Figures 25, 26, 27 and 28 for 3PR, 3BPR, 6PR and 6BPR, respectively. Note that P3 is the front pile and P1 is the rear pile for positive loading, and vice versa for negative loading.

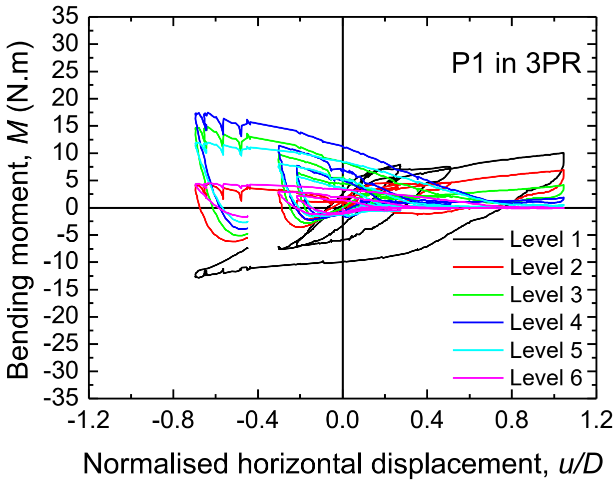

(a)

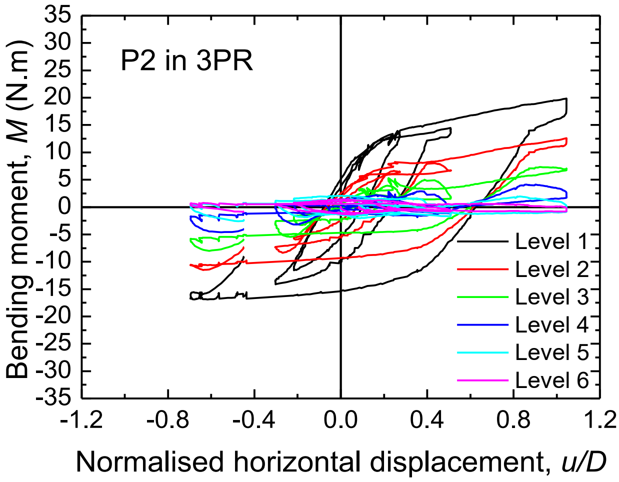

(b)

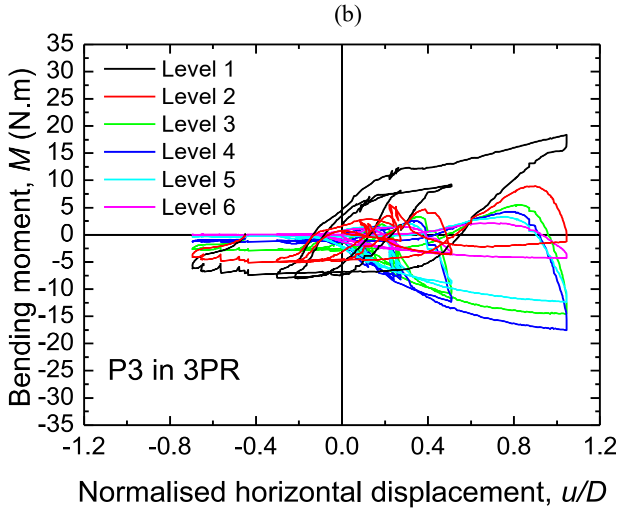

(c)

Figure 25 Bending moments of piles for 3PR (in HLT)

As for the piled rafts without batter piles (3PR and 6PR), the largest magnitudes of bending moments in the front piles and in the centre piles are similar, and higher than those in the rear piles. The magnitudes of bending moments in the centre piles are similar between positive loading and negative loading.

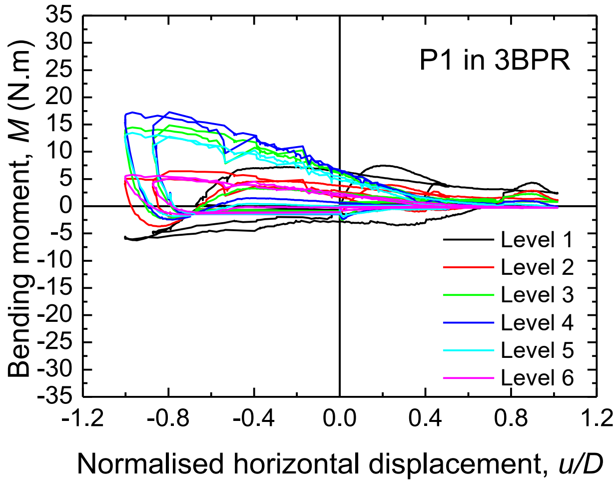

(a)

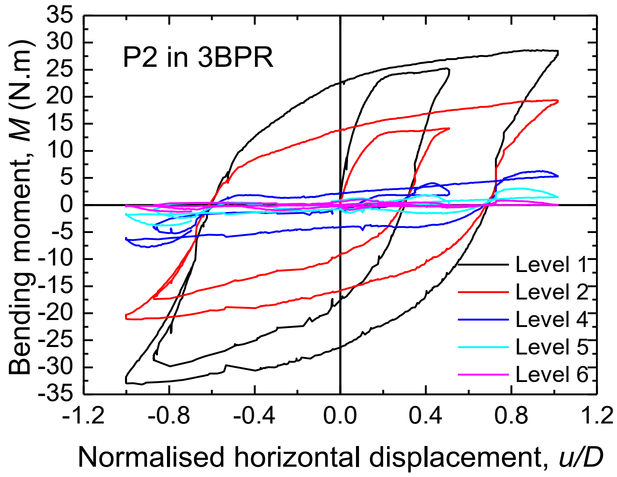

(b)

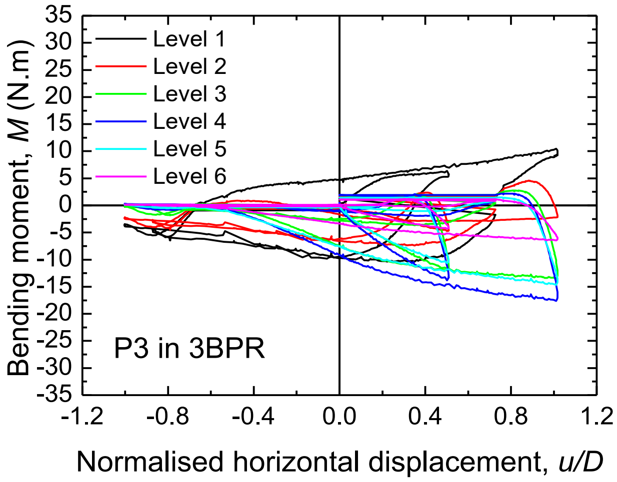

(c)

Figure 26 Bending moments of piles for 3BPR (in HLT)

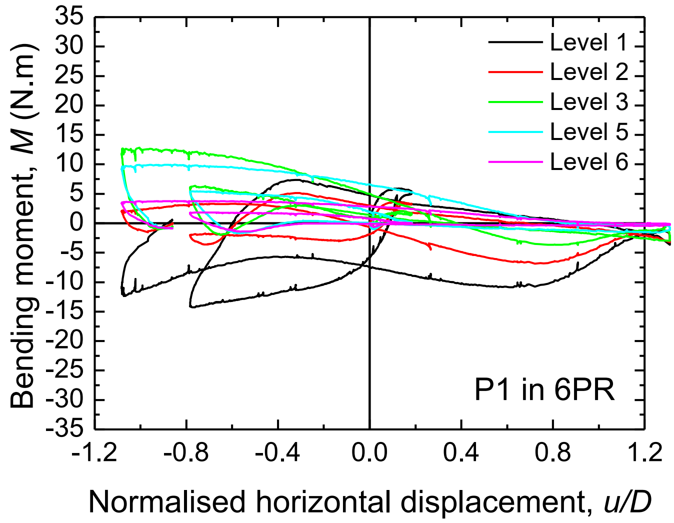

(a)

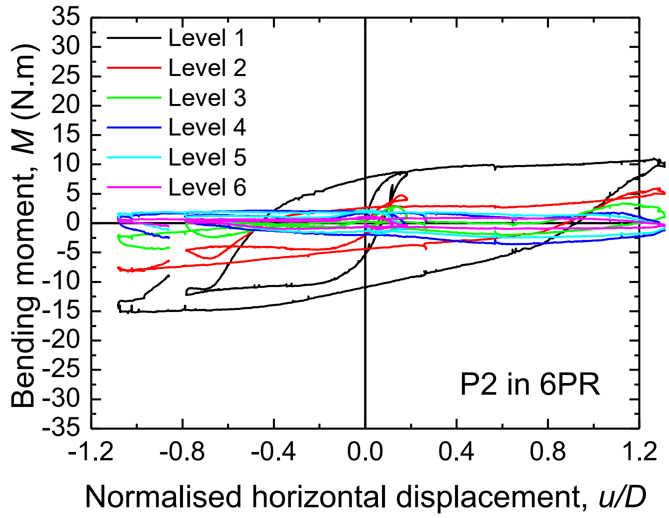

(b)

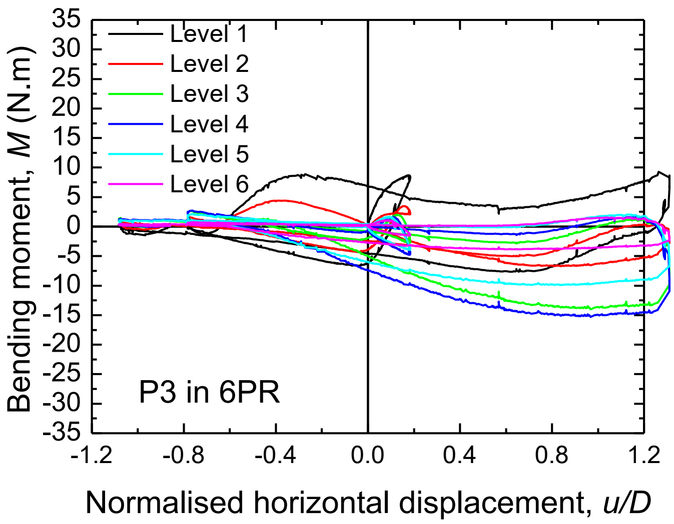

(c)

Figure 27 Bending moments of piles for 6PR (in HLT)

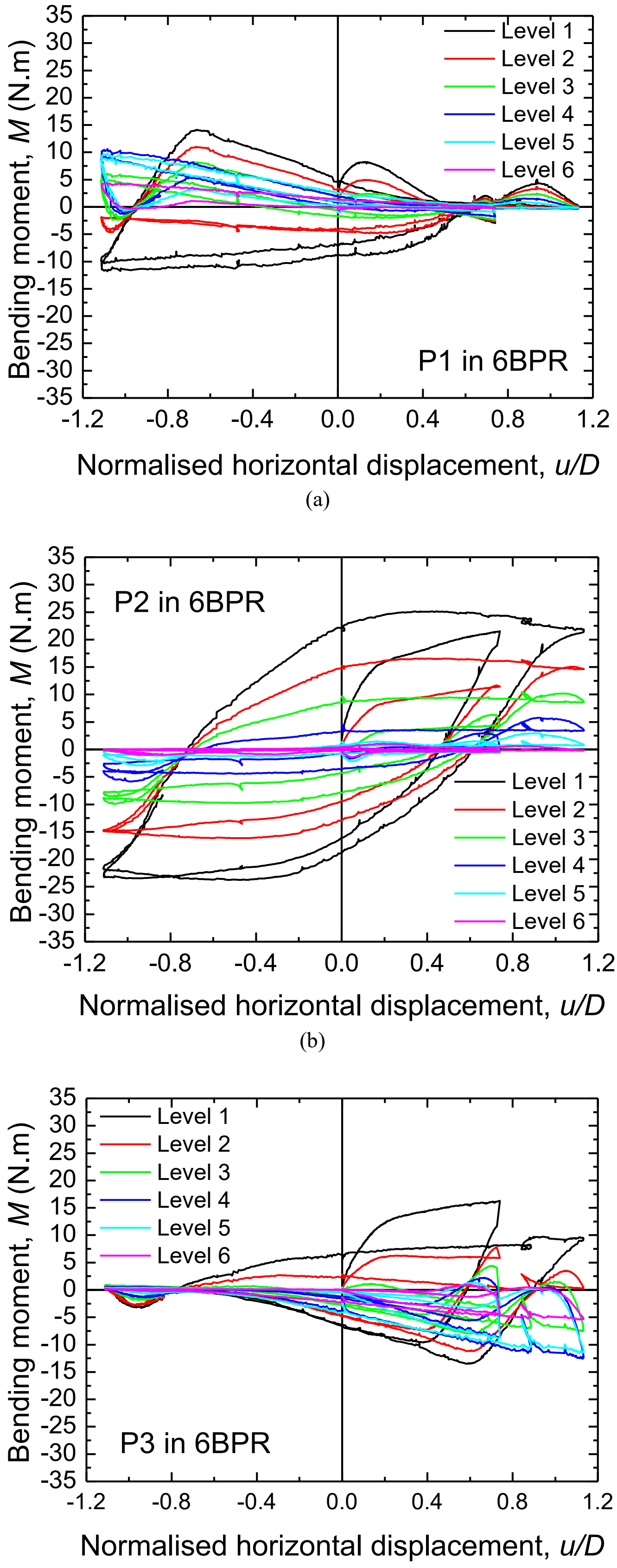

(a)

(b)

(c)

Figure 28 Bending moments of piles for 6BPR (in HLT)

In the centre piles, the maximum bending moments occur at the top of the piles (level 1). In the front piles, the maximum magnitudes of bending moments are generated at the level 1 (top of pile) and the level 4 (distance 140 mm from raft base).

It is obviously seen from Figure 26 and Figure 28 (for 3BPR and 6BPR) that significantly larger bending moments are generated in the vertical centre piles (P2) compared to the other piles (P1 and P3). The bending moments in P2 of 3BPR and 6BPR are also considerably larger than those in P2 of 3PR and 6PR, correspondingly. The bending moments in P1 and P3 of 3BPR and 6BPR are not so much different from those in P1 and P3 of 3PR and 6PR, correspondingly.

Therefore, the increases of axial forces in the batter piles P1 and P3 as well as the increases of the bending moments in the vertical centre pile P2 of 3BPR and 6BPR compared to those in 3PR and 6PR, correspondingly, contribute to enhance the horizontal resistances and to reduce the inclination of the batter pile foundations.

4. CONCLUSIONS

Series of vertical load tests and combination load tests on 3-pile foundation models and 6-pile foundation models (with or without batter piles) in dry sand were carried out at 1-g field to investigate the behaviours and resistance mechanisms of the pile foundations. Triaxial tests of the sand were conducted to obtain the mechanical properties and to investigate to the behaviour of the sand.

It was confirmed from the experiment results of this particular research that the piled raft having batter piles is the most effective foundation type to increase the resistances (in both vertical and horizontal directions) and reduce the inclination.

Batter piles play important role in increasing the resistances and reducing settlement and inclination of the batter pile foundations. In the cases of the pile groups, settlement is significantly reduced by inclusion batter piles.

In the cases of the piled rafts, the raft is an important member to support the load and also plays a very important role in the interaction of raft-soil-pile. The pressure transferred from the raft base to ground increases the resistance of the piles.

The results also indicated that the resistances of the 6-pile foundations are not equal two times the resistances of the corresponding 3-pile foundations, which are effected by interactions between the components of the foundations (piles, raft) and the ground.

Numerical studies would be useful to get deeper insight into the complicated interactions observed in this research. This aspect is our future study.

5. ACKNOWLEGEMENTS

The authors thank the Japanese Society for the Promotion of Science for the financial support (the Grants-in-aid for Scientific Research No. 15K06208). The authors greatly appreciate also Mr. Ryo Yoshitani and Mr. Ahmad Zulhilmi Zainuddin, former students of Kanazawa University, for their supports in carrying out the experiments.

6. REFERENCES

Ghasemzadeh, H., and Alibeikloo, M. (2011) “Pile soil pile interaction in pile groups with batter piles under dynamic loads”. Soil Dynamics and Earthquake Engineering, 31, pp1159-1170.

Goit, CS., and Saitoh, M. (2013) “Model tests and numerical analyses on horizontal impedance functions of inclined single piles embedded in cohesionless soil”. Earthquake engineering and engineering vibration, 12, pp143-154.

Hamada, J., Tsuchiya, T., Tanikawa, T., and Yamashita, K. (2015) “Lateral loading tests on piled rafts and simplified method to evaluate sectional forces of piles”. Geotechnical Engineering Journal SEAGS & AGSSEA, 46(2), pp29-42.

Horikoshi, K., and Randolph, M. F. (1998) “A contribution of optimum design of piled rafts”. Géotechnique, 48(3), pp301-317.

Horikoshi, K., and Randolph, M. F. (1999) “Estimation of overall settlement of piled rafts”. Soils and Foundations, 39(2), pp59-68.

Horikoshi, K., Matsumoto, T., Hashizume, Y., Watanabe, T., and Fukuyama, H. (2003) “Performance of piled raft foundations subjected to static horizontal loads”. Int. Jour. of Physical Modelling in Geotechnics, 3(2), pp37-50.

Iai, S. (1989) “Similitude for shaking table tests on soil-structure-fluid model in 1g gravitational field.” Soils and Foundations, 29(1), pp105-118.

Isam, S., Hassan, A., and Mhamed, S. (2012) “3D elastoplastic analysis of the seismic performance of inclined micropiles”. Computers and Geotechnics, 39, pp1-7.

Katzenbach, R., Arslan, U., and Reul, O. (1998) “Soil-structure-interaction of a piled raft foundation of a 121 m high office building on loose sand in Berlin”. In Proceedings of Deep Foundation on Bored and Auger Piles, pp215-221.

Matsumoto, T., Fukumura, K., Pastsakorn, K., Horikoshi, K., and Oki, A. (2004) “Experimental and analytical study on behaviour of model piled rafts in sand subjected to horizontal and moment loading”. International Journal of Physical Modelling in Geotechnics, 4(3), pp1-19.

Poulos, H.G. and Davids, A.J. (2005) “Foundation design for the Emirates Twin Towers, Dubai”. Canadian Geotechnical Journal, 42, pp716-730.

Poulos, H.G., and Small, J.C., Chow, H. (2011) “Piled raft foundations for tall buildings”. Geotechnical Engineering Journal SEAGS & AGSSEA, 46(2), pp78-84.

Randolph, M. F. (1994) “Design methods for pile groups and piled rafts”. Proc. 13th ICSMGE, Vol. 5, New Delhi, pp. 61-82.

Reul, O. (2004) “Numerical study of the bearing behaviour of piled rafts”. International Journal of Geomechanics, 4(2), pp59-68.

Sadek, M., and Isam, S. (2004) “Three dimensional finite element analysis of the seismic behaviour of inclined micropiles”. Soil Dynamics and Earthquake Engineering 24: 473-485.

Sawada, K., and Takemura, J. (2014) “Centrifuge model tests on piled raft foundation in sand subjected to lateral and moment loads”. Soils and Foundations, 54(2), pp126-140.

Unsever, Y.S., Matsumoto. T., Shimono, S., and Ozkan, M.Y. (2014) “Static cyclic load tests on model foundations in dry sand”. Geotechnical Engineering Journal SEAGS & AGSSEA, 45(2), pp40-51.

Unsever, Y.S., Matsumoto, T., and Ozkan, M.Y. (2015). “Numerical analyses of load tests on model foundations in dry sand”. Computers and Geotechnics, 63, pp40-51.

Vu, A.T., Pham. D.P., Nguyen, T.L., Yu, H. (2014) “3D finite element analysis on behaviour of piled raft foundations”. Applied Mechanics and Materials, Vols. 580-583, pp3-8.

Vu, A.T., Matsumoto, T., Kobayashi, S., and Nguyen, T. L. (2016) "Model load tests on battered pile foundations and finite-element analysis". International Journal of Physical Modelling in Geotechnics (published online Nov 30th 2016), http://dx.doi.org/10.1680/jphmg.16.00010.

Yamashita, K., Yamada, T., and Hamada, J. (2011) “Investigation of settlement and load sharing on piled rafts by monitoring full-scale structures”. Soils and Foundation, 51(3), pp513-532.